Temperature-induced crossover between 0 and π states in S/F/S junctions

Hermann Sellier,* Claire Baraduc, François Lefloch, and Roberto Calemczuk
Département de Recherche Fondamentale sur la Matière Condensée, CEA-Grenoble, 17 rue des Martyrs, 38054 Grenoble, France
(Received 6 May 2003; published 26 August 2003)

Ferromagnetic Josephson junctions can show at equilibrium a π phase difference between the superconducting electrodes. We explain this π state in an original way by a modified spectrum of Andreev bound states shifted by the exchange energy. A simplified expression for the spectral supercurrent density is calculated and the nonmonotonic temperature dependence of the critical current is discussed. This model accounts for the cancellation of the critical current with temperature observed in a small range of barrier thickness in our $Nb/Cu_{52}Ni_{48}/Nb$ junctions. This cancellation corresponds to an inversion of the supercurrent and to a ground-state crossover from a 0 state to a π state. This transition is caused both by the thermal distribution of quasiparticles and by the temperature dependence of the exchange energy. The experimental curves are well reproduced by our theoretical expression except for the very small amplitude of the supercurrent attributed to a large spin-flip scattering.

DOI: 10.1103/PhysRevB.68.054531 PACS number(s): 74.50.+r, 74.45.+c

I. INTRODUCTION

A Josephson junction at equilibrium has usually a phase difference $\phi_{gs}=0$ between the two superconductors, this property being related to the positive coefficient of the current-phase relation. A mechanism leading to a negative coefficient and a ground state with $\phi_{gs}=\pi$ was first proposed in S/I/S junctions with magnetic impurities in the barrier,[1] but any experimental evidence of this effect has never been obtained. Then S/F/S junctions were also predicted to produce π states for an appropriate ratio between the thickness dependent Thouless energy and the exchange energy of the ferromagnetic layer.[2,3]

The experimental study of S/F/S multilayers started with the use of high Curie temperature ferromagnets[4] and a signature of the π state was searched for in the ferromagnetic thickness dependence of the critical temperature. Nonmonotonic behaviors of T_c were observed and attributed either to the π state[5] or to the onset of ferromagnetism.[6] These experiments are indeed difficult to interpret because the large values of the exchange energy require very thin layers for which ferromagnetic properties are strongly thickness dependent. The conclusions of these studies regarding the existence of the π state remain controversial.

Recently, perpendicular transport measurements through the ferromagnetic barrier have been carried out on S/F/S Josephson junctions with low Curie temperature ferromagnets. Ryazanov *et al.* observed a nonmonotonic temperature dependence of the critical current in Nb/CuNi/Nb junctions interpreted as a crossover between a 0 state and a π state.[7] They also placed five of these junctions in a double loop interferometer and observed a shift of half a flux quantum in the interference pattern.[8] These results provide the first unambiguous proof of the existence of the π state. More recently similar results have been obtained in $Nb/Al_2O_3/PdNi/Nb$ junctions using the ferromagnetic thickness dependence instead of the crossover in temperature which has not been observed.[9,10]

This paper presents both a theoretical analysis and an experimental study of the transition between the 0 state and the π state in S/F/S junctions. In Sec. II we give an alternative explanation of the π state based on the Andreev bound-states spectrum instead of the superconducting correlation function considered in the previous works. The origin of the supercurrent in S/N/S junctions derives indeed from the existence of these bound states in the normal metal.[11] The ''sign'' of the supercurrent can be directly deduced from the dependence of the Andreev spectrum with the phase difference. This approach therefore provides an intuitive understanding of the ''negative sign'' of the critical current in S/F/S junctions responsible for the π state. For clarity we will first consider the ballistic and one-dimensional case because the Andreev spectrum is easier to describe.

However, the experimental devices are in the diffusive regime and the distribution of Andreev bound states becomes more complicated. The significant quantity is the spectral supercurrent density which is closely related to the Andreev spectrum of the ballistic case. This function gives the supercurrent carried by the Andreev bound states at a given energy and was originally introduced to analyze nonequilibrium situations.[12] In Sec. III we calculate this spectral supercurrent density for S/F/S junctions using the linearized Usadel equations and explain the ''negative'' critical current by an unusual *spectral* behavior instead of a *spatial* oscillation of the superconducting correlation function.

We also consider the spectral approach instead of the Matsubara formalism in order to clarify the temperature dependence of the supercurrent which is very unusual in S/F/S junctions. It should be noticed that the early theoretical works neglected the influence of temperature on the pair density in the ferromagnetic region because the experimental studies focused only on large Curie temperature ferromagnets. The investigation of low exchange energies is recent and the nontrivial influence of the temperature which can reverse the sign of the supercurrent requires a deeper analysis. This behavior has no obvious physical interpretation in the Matsubara formalism whereas the spectral approach provides a simple explanation.[13]

In Sec. IV we present our experimental study of $Nb/Cu_{52}Ni_{48}/Nb$ junctions with barrier thicknesses close to

the value inducing a crossover between the 0 state and the π state. The critical current of these junctions has a nonmonotonic temperature dependence with a complete cancellation at a temperature which depends on the thickness. This cancellation actually corresponds to the sign change of the current-phase relation coefficient discussed in the theoretical part and whose consequence is a switch from the 0 state to the π state. This very unusual temperature dependence is the same as the one reported by Ryazanov *et al.*[7] However, they used a different copper-nickel alloy with a ferromagnetic behavior, whereas our alloy is nearly superparamagnetic. Measurements of the critical current as a function of the magnetic field show typical Fraunhofer patterns centered around zero field at all temperatures. This confirms that the vanishing supercurrent is an intrinsic property of our S/F/S junctions and is not due to magnetic induction.

This interpretation as a 0 to π crossover is also supported by a comparison in Sec. V between the experimental data for different barrier thicknesses and the theoretical expression of the critical current calculated in Sec. III. We include the contribution of the temperature-dependent exchange energy because the measured magnetization does not saturate at low temperature. The extremely small amplitude of the supercurrent cannot be accounted for by the theoretical expression in its simplest formulation. It can however be reproduced if we include a strong spin-flip scattering which may be present in our superparamagnetic copper-nickel alloy.

II. EXPLANATION OF THE π STATE USING THE ANDREEV BOUND STATES

A. S/N and S/F proximity effect

The wave function of the superconducting condensate at zero temperature is a coherent superposition of partially occupied states in the energy range of the gap Δ around the Fermi level as can be seen from the BCS expression.[14,15] Some of these states have therefore a wave vector above the Fermi level and can be injected in the normal metal at the S/N interface (see Fig. 1). However, electrons can only be removed by pairs in a superconductor, so that a second electron has to leave the condensate and it fills a hole state below the Fermi level in N. From the superconductor point of view, two electrons have been transferred from S to N, and from the normal-metal point of view, a hole in N has been reflected into an electron in N. This mechanism of charge transfer at the S/N interface is called an Andreev reflection.[16] The symmetric case is also involved in which an electron above the Fermi level in N cross the S/N interface and a hole is left (Andreev reflected) below the Fermi level in N.

We discuss now the phase coherence of an electron and a hole correlated by an Andreev reflection. At the Fermi level, the two particles have the same wave vector $k_e = k_h$ and follow exactly the same path with opposite group velocities. The relative phase of their wave functions is constant along this path and the coherence length of the pair is very long (limited by the phase breaking length L_φ). If the electron is at finite energy $0 < \epsilon < \Delta$ with a wave vector $k_e(\epsilon) = k_F + \delta k$ where $\delta k = \epsilon/\hbar v_F$, the hole has the same energy ϵ but below the Fermi level and has therefore a smaller wave vector $k_h(\epsilon) = k_F - \delta k$. This difference produces a relative phase shift in the Andreev pair equal to $2\delta k\, x$. This shift reduces the coherence length in the diffusive regime because the elastic diffusions scatter the two particles differently when their phase difference becomes larger than unity (or equivalently when the particles become separated by more than a Fermi wavelength).

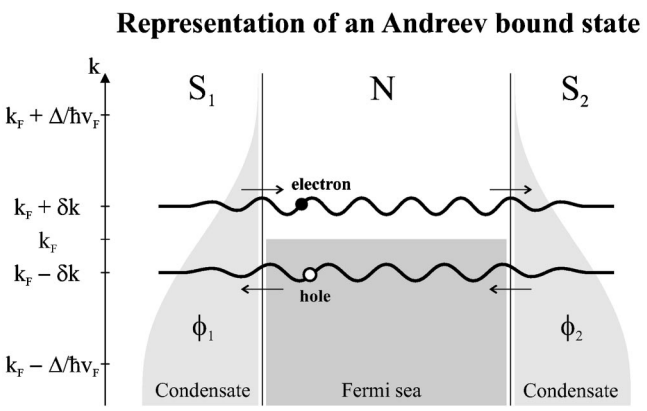

FIG. 1. Electron and hole wave functions of an Andreev pair which forms a bound state in an S/N/S junction. The gray areas represent the distribution of occupied states at zero temperature. An electron is injected from the superconductor into the normal metal above the Fermi level and a hole is captured below at the same time. A bound state is formed when the wave functions satisfy the boundary conditions imposed by the superconducting phases ϕ_1 and ϕ_2.

In a ferromagnetic metal, the two spin subbands are split by the exchange energy $\pm E_{ex}$ and they have Fermi wave vectors equal to $k_F \pm q$ where $q = E_{ex}/\hbar v_F$. Because the electron and the hole of an Andreev pair are in opposite spin subbands, their wave vectors are now equal to

$$\begin{cases} k_e^{\downarrow}(\epsilon) = k_F - q + \delta k, \\ k_h^{\uparrow}(\epsilon) = k_F + q - \delta k, \end{cases}$$

and

$$\begin{cases} k_e^{\uparrow}(\epsilon) = k_F + q + \delta k, \\ k_h^{\downarrow}(\epsilon) = k_F - q - \delta k, \end{cases} \tag{1}$$

for the two types of pairs.[17] At the Fermi level, they have a phase shift $2qx$ which is responsible for a short coherence length $\xi_F = \sqrt{\hbar D/E_{ex}}$ in the diffusive regime. However at the particular value $\epsilon = E_{ex}$, the excitation energy for pairs with spin-down electrons is exactly compensated by the exchange energy because $\delta k = q$. The wave vectors $k_e^{\downarrow}(E_{ex})$ for the electron and $k_h^{\uparrow}(E_{ex})$ for the hole are both equal to k_F and the internal phase shift disappears. A long coherence length can therefore be recovered in case of a small exchange energy $E_{ex} < \Delta$.

B. Andreev bound states in S/N/S junctions

In a ballistic normal metal placed between two superconducting electrodes, the Andreev reflections at the two interfaces create discrete bound states.[18] The spectrum of these levels is sensitive to the superconducting phase difference between the electrodes $\phi=\phi_2-\phi_1$ as described in the following.[11,19–21] The wave function of an Andreev state at energy $0<\epsilon<\Delta$ is evanescent in S and propagates in N (see Fig. 1). At the S_1/N (N/S_2) interface, the relative phase $\varphi=\varphi_e-\varphi_h$ between the electron and hole components is equal to the macroscopic phase ϕ_1 (ϕ_2) of the superconductor, plus an additional term $-(+)\arccos\epsilon/\Delta$ due to the evanescent part of the wave in S. In a ballistic and one-dimensional S/N/S junction, going from one interface to the other, the relative phase of the pair changes by $\Delta\varphi=2\delta k\, d$, where d is the length of normal metal and $\delta k=\epsilon/\hbar v_F$. A bound state appears at energy ϵ_n if this phase shift $\Delta\varphi$ matches the phase difference at the two interfaces, modulo 2π. For a pair with a wave vector in the opposite direction, the phases ϕ_1 and ϕ_2 have to be exchanged. The discrete Andreev bound states for positive and negative wave vectors are given by

$$\Delta\varphi=2\frac{\epsilon_n}{\hbar v_F}d=\pm\phi+2\arccos\frac{\epsilon_n}{\Delta}+2\pi n. \qquad (2)$$

There is no state at $\epsilon=0$ for $\phi=0$ because there is no phase shift during the transport across the normal metal whereas the phase difference imposed by the two interfaces should be equal to π. At $\epsilon=\Delta$ no phase shift is required and a bound state is possible even for a very short junction where $\Delta\varphi=0$. Two successive levels are separated by πE_{Th} (for $\epsilon\ll\Delta$) where $E_{Th}=\hbar v_F/d$ is the Thouless energy. At zero temperature, electrons can be injected above the Fermi level from the superconducting electrodes thanks to the distribution of occupied states in the condensate. The corresponding holes of the pairs are below the Fermi level and carry currents in the same direction because they have opposite charge and group velocity. An Andreev state with $k>0$ carries a charge $-2e$ in the direction of its wave vector and therefore a negative current. For this reason we call $(-)$ the states $k>0$ and $(+)$ the states $k<0$. For $\phi=0$, the $(+)$ and $(-)$ states are degenerate and there is no resulting current. For $\phi>0$, the energy of the $(+)$ states decreases, whereas the energy of the $(-)$ states increases, and the spectrum alternates levels with opposite currents as shown in Fig. 2(a). Since the lowest levels are the most occupied, the normal metal carries a finite and positive current which is called ''supercurrent'' because no voltage is required. An important point to remember for the following is that the direction of the total current is given by the first level. The current is maximum for $\phi=\pi^-$ when this first level reaches $\epsilon=0^+$. For $\phi=\pi^+$ this $(+)$ level disappears and a $(-)$ level appears at $\epsilon=0^+$. As a result, the current-phase relation shown in Fig. 3(a) is a 2π-periodic function with a sawtooth shape at zero temperature in this ballistic regime.

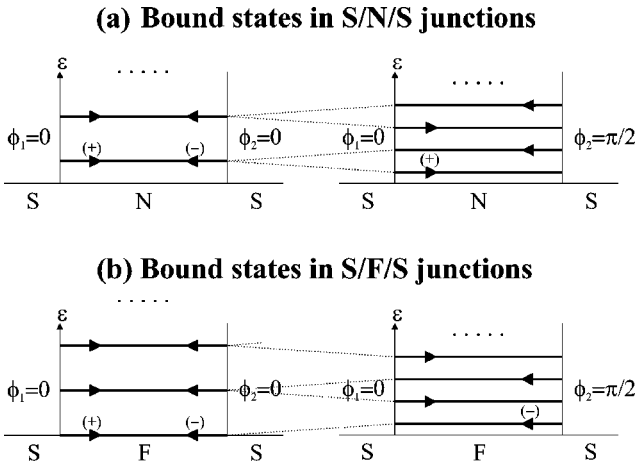

FIG. 2. Discrete spectrum of Andreev bound states in a long one-dimensional ballistic (a) S/N/S junction and (b) S/F/S junction with $E_{ex}=(\pi/2)E_{Th}$. Each degenerate state is split by the phase difference $\phi=\pi/2$ into states carrying currents in opposite directions. The first state above the Fermi level has the largest contribution to the total supercurrent which is positive for the S/N/S junction and negative for the S/F/S junction.

C. Andreev bound states in S/F/S junctions

In ferromagnetic junctions, the phase shift of the Andreev pairs contains the additional term $\pm 2qd$ due to the exchange energy and Eq. (2) has to be changed into

$$\Delta\varphi=2\frac{\epsilon\pm E_{ex}}{\hbar v_F}d=\pm\phi+2\arccos\frac{\epsilon}{\Delta}+2\pi n. \qquad (3)$$

For the $(\uparrow\downarrow)$ pairs with a *spin-up* electron and a *spin-down* hole, the additional phase shift is positive and thus the bound

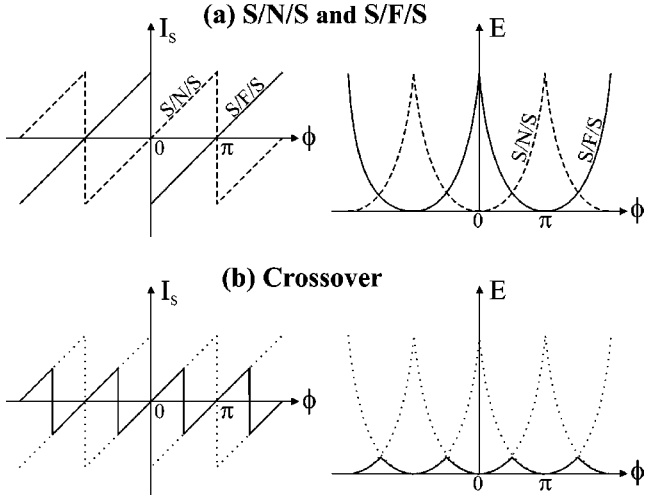

FIG. 3. (a) Current-phase relation at zero temperature and the corresponding energy-phase relation for a long one-dimensional ballistic S/N/S junction and for an S/F/S junctions with $E_{ex}=(\pi/2)E_{Th}$. The ground states are, respectively, the 0 state with $\phi_{gs}=0$ and the π state with $\phi_{gs}=\pi$. (b) These two states are degenerate at the crossover for $E_{ex}=(\pi/4)E_{Th}$, but the critical current is nonzero.

states move to lower energies. Similarly, for the $(\downarrow\uparrow)$ pairs, they move to higher energies. Each level is therefore split into its two spin components.

In the following, we consider the particular value $E_{ex}=(\pi/2)E_{Th}$ and analyze the modification of the Andreev spectrum as shown in Fig. 2(b). For $\phi=0$ the first level $(\uparrow\downarrow)$ is shifted from $(\pi/2)E_{Th}$ to 0 because the additional phase shift $2qd$ gives exactly the appropriate value $\Delta\varphi=\pi$ to match the boundary conditions with the superconductors. When the phase difference ϕ increases, the $(+)$ state disappears immediately below the Fermi level and the $(-)$ state rises above carrying a current in the negative direction. This shifted spectrum with an Andreev bound state at zero energy is therefore responsible for a negative supercurrent at positive phase difference.

The current-phase relation and also the energy-phase relation given by $dE/d\phi=(\hbar/2e)I_S$ are translated by π compared to the normal case as shown in Fig. 3(a). The minimum of the energy corresponding to the ground state is obtained for $\phi_{gs}=\pi$ (instead of $\phi_{gs}=0$ for normal case) and this S/F/S junction is therefore called a π junction. This description using the Andreev bound states shifted by the exchange energy provides from our point of view a deeper understanding of the origin of the π state than the previous works on this subject.

The Andreev spectrum *in this π ground state* is obtained by setting $\phi=\pi$ in Eq. (3) and is therefore identical to the spectrum of an S/N/S junction with $E_{ex}=0$ and $\phi_{gs}=0$. The additional phase shift $2qd=\pi$ is compensated by the phase difference $\phi_{gs}=\pi$. In particular the first bound state is not at $\epsilon=0$. The situation would be different in an S/F bilayer because this system corresponds to an S/F/S junction always at $\phi=0$ (and two times thicker). As a result, the density of state which is always minimum at $\epsilon=0$ in S/N systems can be maximum at $\epsilon=0$ in the S/F case because of the shifted bound states. This ''reversed'' density of states has been observed experimentally in diffusive Nb/PdNi bilayers.[22]

Finally we briefly discuss the situation of an exchange energy equal to $(\pi/4)E_{Th}$. The level spacing of the Andreev bound states for $\phi=0$ is two times smaller and the current-phase relation has a period of π as shown in Fig. 3(b). The 0 state and the π state are degenerate but the critical current is nonzero at the crossover in this ballistic regime.

III. TEMPERATURE-INDUCED CROSSOVER IN DIFFUSIVE REGIME

A. Spectral supercurrent in S/N/S junctions

In the diffusive regime the Andreev bound states have a continuous distribution and induce a spectral supercurrent density $N_J(\epsilon)$ in the normal metal.[12,23] In the following, we derive a simplified expression for $N_J(\epsilon)$, by first calculating the supercurrent in the Matsubara formalism and then by transforming the expression in real time formalism.

The nonlinear Usadel equations[24] for the Green functions $G(\omega_n,x)$ and $F(\omega_n,x)$ can be solved by numerical calculation in the general case. However for a better analysis of the result, an analytical expression for the supercurrent is more convenient, but requires some approximations. We suppose a small amplitude of the induced correlations in the normal metal and linearize the equations with $G\approx 1$ and $F\ll 1$. In principle, this approximation is only valid for temperatures larger than the gap, close to the superconducting transition. However, it can also be used at all temperatures for the calculation of the supercurrent if the exact numerical values are not needed. We also assume a perfect transparency of the S/N interfaces at $x=\pm d/2$ and do not solve self-consistently the order parameter in the superconductors. We calculate the supercurrent as done in Ref. 25 using the following equations where $\omega_n=(2n+1)\pi k_B T$:

$$I_S(T)=\frac{2\pi k_B T}{e R_N}\sum_{\omega_n>0}\mathrm{Im}[d F^*\nabla F] \tag{4}$$

$$-\frac{\hbar D}{2}\nabla^2 F+\omega_n F=0, \tag{5}$$

$$F(\pm d/2)=\frac{\Delta}{\sqrt{\Delta^2+\omega_n^2}}e^{\pm i\phi/2}. \tag{6}$$

In real time formalism, the supercurrent is expressed as an integral over the energies ϵ instead of a sum over the Matsubara frequencies ω_n. The spectral supercurrent density $N_J(\epsilon)$ corresponds to the term in the sum in Eq. (4) where ω_n is replaced by $-i(\epsilon+i\gamma)$. The parameter $\gamma=0^+$ suppresses the singularities and comes from the retarded Green functions involved in the spectral densities. In this formalism the supercurrent is now given by the following expressions (γ is removed when not necessary):

$$I_S(T)=\frac{1}{e R_N}\int_0^{+\infty}N_J(\epsilon)\,h(\epsilon)d\epsilon, \tag{7}$$

$$N_J(\epsilon)=\mathrm{Im}\left[\frac{\Delta^2}{\Delta^2-(\epsilon+i\gamma)^2}\frac{\sqrt{-2i\epsilon/E_{Th}}}{\sinh\sqrt{-2i\epsilon/E_{Th}}}\right]\sin\phi, \tag{8}$$

$$h(\epsilon)=1-2f_T(\epsilon)=\tanh(\epsilon/2k_B T). \tag{9}$$

The spectral supercurrent density is plotted in Fig. 4(a) in the long junction case $E_{Th}\ll\Delta$ with a Thouless energy in the diffusive regime $E_{Th}=\hbar D/d^2$. Only positive energies have a physical meaning but we also plot the function for negative energies to simplify the transition to the S/F/S case. The oscillations correspond to the previously discussed $(+)$ and $(-)$ discrete bound states split by the phase difference $\phi=\pi/2$ and carrying the current in opposite directions. The exponential decay comes from the diffusive regime where the coherence of the Andreev states at energy ϵ is broken beyond a characteristic length $l_\epsilon=\sqrt{\hbar D/\epsilon}$. The linearization of the equations is responsible for the absence of a minigap around E_{Th} and for a current-phase relation proportional to $\sin\phi$. The critical current is obtained for $\phi=\pi/2$.

At zero temperature, all the states are available and the total supercurrent is the integral of $N_J(\epsilon)$. At finite temperature, quasiparticle states are occupied by thermal excitations

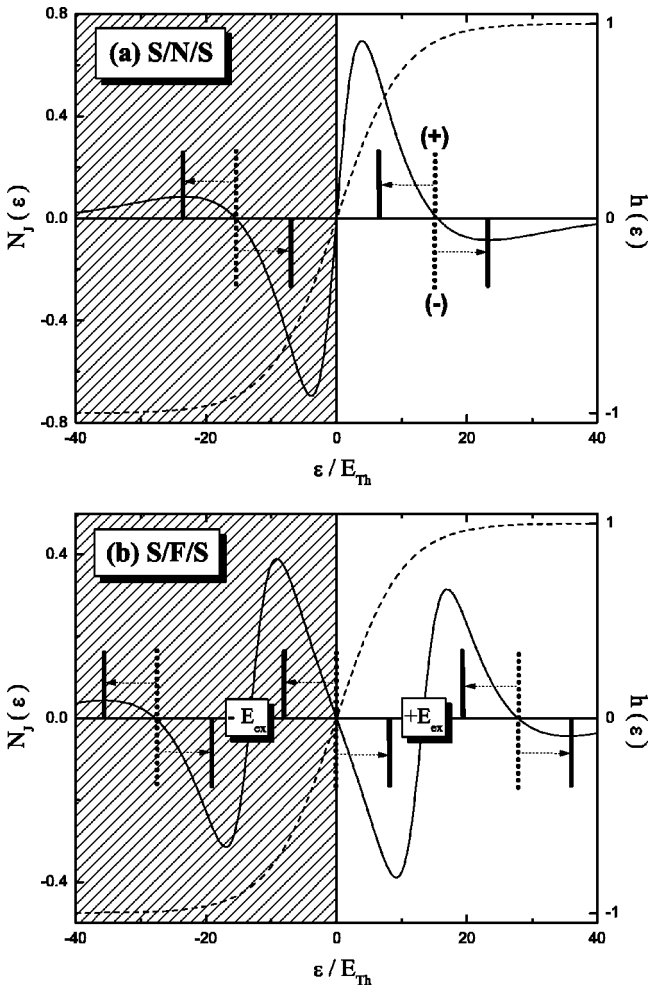

FIG. 4. Spectral supercurrent density for $\phi=\pi/2$ (solid line) and distribution function for $k_BT=5\,E_{Th}$ (dashed line) in long (a) S/N/S junction and (b) S/F/S junction with $E_{ex}=13E_{Th}\ll\Delta$. The vertical bars illustrate the relation with the discrete Andreev bound states of the ballistic regime: the $(+)$ and $(-)$ states carrying currents in opposite directions are split by the phase difference. In the S/F/S case the two spin components of the spectral density are shifted by $\pm E_{ex}$. Only the positive energies have a physical meaning and enter in Eq. (7).

according to the Fermi distribution $f_T(\epsilon)$. The available energies for the coherent Andreev bound states are above these excitations and are given by the function $h(\epsilon)$. Some Andreev levels are therefore suppressed and the supercurrent decreases with increasing temperature in a monotonic way as shown in Fig. 5.

The oscillations of the spectral supercurrent density have been taken advantage of to change the sign of the Josephson current.[26] A transverse voltage is applied to the mesoscopic normal metal of an S/N/S junction at low temperature and an out-of-equilibrium distribution function with two sharp steps is produced. For a voltage equal to the first node of $N_J(\epsilon)$, the large positive contribution is suppressed, whereas the small negative one at higher energy is still fully active and the sign of the total supercurrent is reversed. The negative supercurrent of ferromagnetic junctions also comes from these oscillations of the spectral supercurrent density, but in a

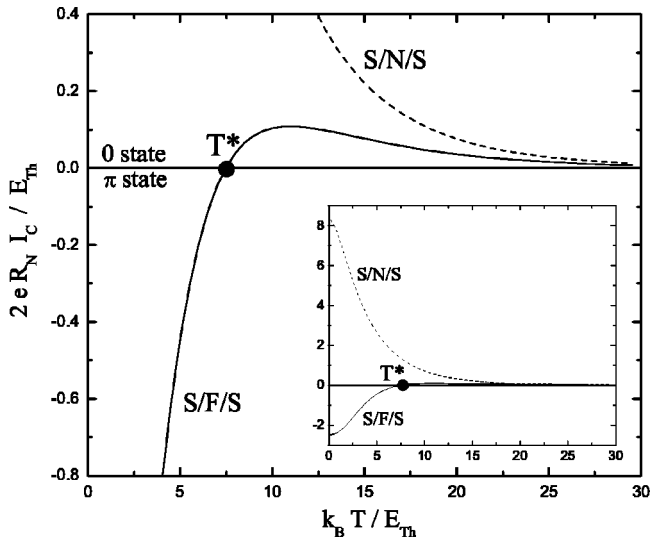

FIG. 5. Crossover between 0 and π states at a temperature T^* resulting from a nonmonotonic dependence of the critical current in a long S/F/S junction with $E_{ex}=13\,E_{Th}\ll\Delta$ (solid line), compared to the monotonic behavior of S/N/S junctions (dashed line). The inset shows the same curves on a larger scale.

different way: the shift of $h(\epsilon)$ induced by the voltage is replaced by a shift of $N_J(\epsilon)$ induced by the exchange energy.

B. Spectral supercurrent in S/F/S junctions

The exchange energy E_{ex} increases or decreases the phase shift of the Andreev pairs and affects not only the position of the bound states but also their coherence in this diffusive regime. This coherence is maximum when the excitation energy of the Andreev pair and the exchange energy compensate each other. The spectral supercurrent density is shifted to higher energy by $+E_{ex}$ for the $(\downarrow\uparrow)$ pairs and to lower energy by $-E_{ex}$ for the $(\uparrow\downarrow)$ pairs. The total supercurrent density is the sum of the two spin contributions:

$$N_J(\epsilon)=\mathrm{Im}\left[\frac{\Delta^2}{\Delta^2-(\epsilon+i\gamma)^2}\left(\frac{\sqrt{-2i(\epsilon+E_{ex})/E_{Th}}}{\sinh\sqrt{-2i(\epsilon+E_{ex})/E_{Th}}}+\frac{\sqrt{-2i(\epsilon-E_{ex})/E_{Th}}}{\sinh\sqrt{-2i(\epsilon-E_{ex})/E_{Th}}}\right)\right]\sin\phi. \tag{10}$$

In the long junction case $E_{Th}\ll\Delta$, the first term containing the gap is close to unity, so that $N_J(\epsilon)$ in the S/F/S case is simply the sum of two shifted functions of the S/N/S case. The corresponding function is shown in Fig. 4(b). The large negative peak which was below the Fermi level in the S/N/S case is now above and gives a negative contribution. This mechanism is the same as in the ballistic case where the first bound state above the Fermi level is a $(-)$ state for $\phi>0$. Since the area of the negative part of the function is slightly larger than that of the positive one, the sign of the total supercurrent I_S is negative at zero temperature and the ground state of the junction is a π state.

At finite temperature, the spectral supercurrent density is multiplied by the distribution function $h(\epsilon)$. The contribu-

tion of the negative part just above the Fermi level is reduced because the Andreev levels at low energy are partially suppressed by the thermal excitations. The positive part becomes dominant and reverses the sign of the total supercurrent. When the temperature is increased, the critical current varies continuously from a negative value to a positive one and changes sign at a crossover temperature T^* as shown in Fig. 5. Such a junction is in the π state at low temperature and in the 0 state above T^*.

It is important to notice that this behavior is possible only in the S/F/S case because the negative and positive contributions of the spectral supercurrent density have nearly the same amplitude. This property is due to the decoherence of the diffusive regime which is canceled at $\epsilon = E_{ex}$ (zero internal phase shift). In the S/N/S case, because the exponential decay is centered at $\epsilon = 0$, the positive part is much larger than the negative one and the supercurrent is always positive as a function of temperature. An out-of-equilibrium situation induced by a voltage is required to obtain an S/N/S π junction as already mentioned.

The additional phase shift of the Andreev pairs due to the exchange energy corresponds to a spatial oscillation of the anomalous Green function $F(\omega_n, x)$ calculated in Matsubara formalism. This function describes the superconducting correlations $\langle \psi_\uparrow(x)\psi_\downarrow(x)\rangle$ in the normal metal, but the intrinsic oscillations due to the excitation energy ϵ are suppressed by an integration at thermal equilibrium. On the other hand, the additional relative momentum $2q$ is identical for all the Andreev pairs and survives to this integration. It induces an oscillatory behavior with a period related to $\xi_F = \sqrt{\hbar D/E_{ex}}$ as explained in Ref. 17. This spatial oscillation can connect the two superconducting order parameters with opposite signs and produce a π state when $d \sim \xi_F$ (equivalent to $E_{Th} \sim E_{ex}$). However, this intuitive explanation[3,7,27] does not explain the electronic process involved in the Josephson coupling. A more physical understanding can be obtained with the Andreev bound states as presented in this paper. Moreover, the spectral approach is necessary to understand the temperature induced crossover between the 0 state and the π state.

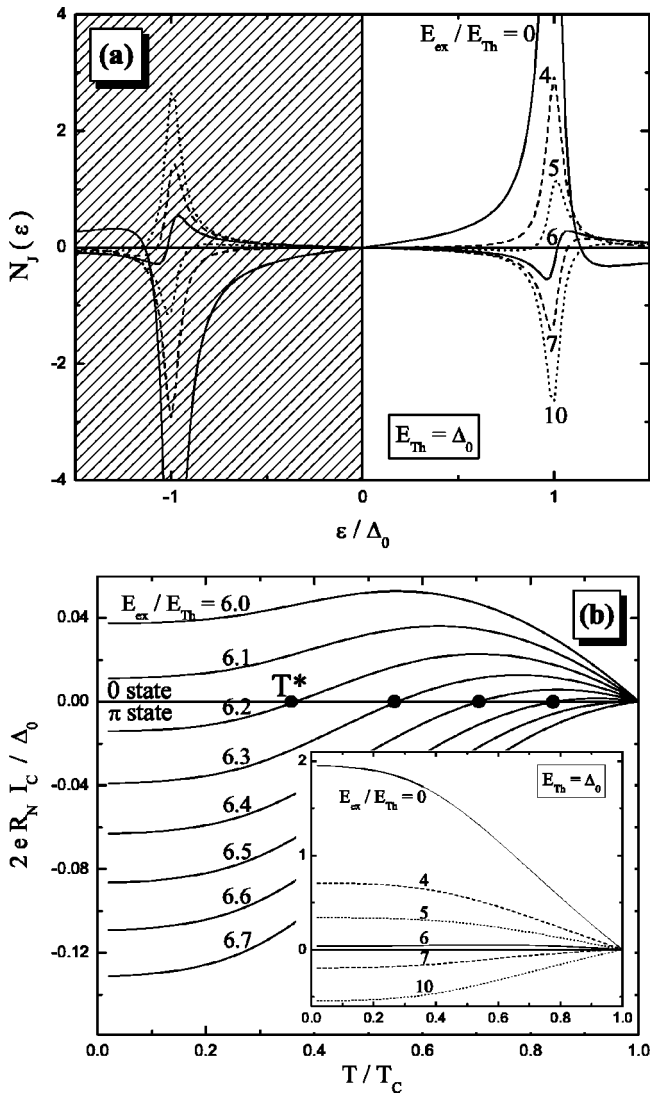

FIG. 6. (a) Spectral supercurrent density for $\phi = \pi/2$ at zero temperature in short junctions with $E_{Th} = \Delta_0$ and different exchange energies $E_{ex}/E_{Th} = 0 - 10$. (b) Temperature dependence of the critical current in the range 6.0–6.7 (and 0–10 in the inset). The temperature induces a crossover between 0 and π states only in the small range 6.2–6.5.

C. Short junction case and large exchange energy

The above analysis was done in the long junction case with $E_{ex} \approx E_{Th} \ll \Delta_0$. We now discuss the case of an intermediate exchange energy $E_{ex} \sim \Delta_0$ corresponding to our experimental situation. A short junction with $E_{Th} \sim \Delta_0$ is therefore required to obtain a π junction with a $0-\pi$ crossover in temperature. When the thickness is decreased, the energy spacing between the Andreev levels increases as shown from Eq. (2) for the bound states in ballistic regime: only one state remains at $\epsilon = \Delta$ for very short junctions. For the same reason the function $N_J(\epsilon)$ in the diffusive regime has a peak around $\epsilon \sim \Delta$. This peak comes from the first term in Eq. (8) which does not contain the exchange energy because it describes the superconductivity in the electrodes. The function $N_J(\epsilon)$ in the S/F/S case is thus no more a shift of the S/N/S case as can be seen in Fig. 6(a) for increasing exchange energies. When the exchange energy and the Thouless energy are of the same order, the large positive peak is replaced by a negative peak corresponding to a shifted Andreev spectrum. The supercurrent becomes negative and the ground state is a π state.

The temperature dependence of the critical current is plotted in Fig. 6(b) using an approximate expression $\Delta(T) = \Delta_0\sqrt{1-(T/T_c)^2}$ for the superconducting gap with the BCS relation $\Delta_0 = 1.76\, k_B T_c$. A π state at zero temperature is obtained for exchange energies in the range $[6.2\, E_{Th}, 31 E_{Th}]$, but a crossover to a 0 state in temperature is obtained only in the interval $[6.2\, E_{Th}, 6.5\, E_{Th}]$. This very narrow range of parameters illustrates the necessity to have an exchange energy as small as possible, at least comparable with the superconducting gap, in order to observe experimentally the crossover in temperature.

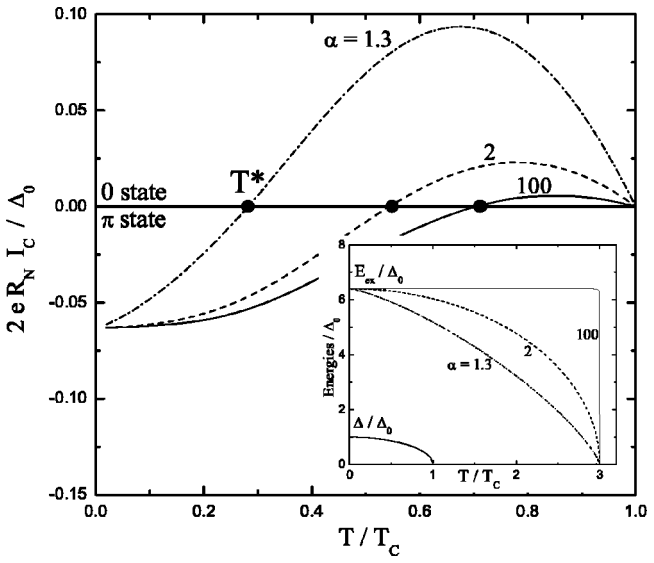

FIG. 7. Crossover in temperature with the additional contribution of a temperature-dependent exchange energy $E_{ex}(T)$ in a short S/F/S junction with $E_{Th}=\Delta_0$, $E_{ex}(0)=6.4\,\Delta_0$, and $T_{Curie}=3\,T_c$. Three different dependencies are compared: $\alpha=100$, 2, and 1.3, corresponding to the increasing temperature variations shown in the inset.

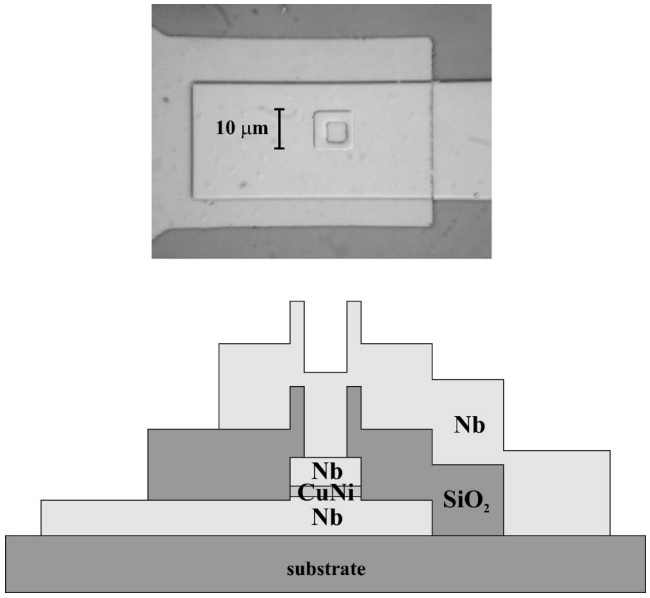

FIG. 8. Photograph and cross section of a device: a square junction of $10\times10\ \mu m^2$ is etched in the $Nb/Cu_{52}Ni_{48}/Nb$ trilayer and the contact is made on the top through a window in a SiO_2 layer.

D. Temperature-dependent exchange energy

In the above description the exchange energy was assumed to be a constant parameter. Its dependence with temperature can no more be neglected if the crossover occurs when the magnetization has not reached its saturation value (if T^* is not much smaller than T_{Curie}). In this case the Andreev spectrum tends to move back towards the position for zero exchange energy when the temperature is increased and the negative critical current tends to become positive again. This effect suggested in Ref. 2 adds to the intrinsic $0-\pi$ crossover we described previously caused by the thermal distribution of quasiparticles.

We illustrate this effect in Fig. 7 by plotting the critical current versus temperature for different variations of the form $E_{ex}(T)=E_{ex}(0)[1-(T/T_{Curie})^{\alpha}]^{1/\alpha}$. The value at zero temperature is fixed at $E_{ex}(0)=6.4E_{Th}$ corresponding to a negative critical current for $E_{Th}=\Delta_0$ and we choose $T_{Curie}=3T_c$ typical for dilute ferromagnetic alloys. For $\alpha=100$, the exchange energy is constant below T_c, so that the crossover is induced by the thermal distribution function only. For $\alpha=2$, the crossover occurs at lower temperature because the two mechanisms are involved. For a faster decrease with $\alpha=1.3$, the temperature dependence of the critical current is almost dominated by the variations of the exchange energy. This additional effect can therefore contribute significantly to the $0-\pi$ crossover.

IV. EXPERIMENTAL STUDY OF $Nb/Cu_{52}Ni_{48}/Nb$ JUNCTIONS

A. Description of the devices

We now present our experimental results on π junctions which support the theoretical analysis of the previous part. The crossover in temperature is easier to observe if the range of temperature is large (high superconducting transition temperature) and if the exchange energy is weak. So we chose niobium for the superconducting electrodes and a dilute copper-nickel alloy for the ferromagnet barrier. The first step of the process is to deposit the three layers Nb(100 nm)/CuNi(15–20 nm)/Nb(100 nm) *in situ* in order to achieve a good quality of the interfaces. The patterning of the planar junctions is then made by photolithography. The bottom electrode is defined in this trilayer by a lift-off process and a square of $10\times10\ \mu m^2$ is then dry etched to define the junction. The contact on the top is made with a Nb electrode through a window in a SiO_2 layer (Fig. 8).

Nb and CuNi are sputtered using dc magnetron sources at room temperature in 1.64×10^{-2} mbar of argon gas. The residual pressure inside the chamber is about 10^{-7} mbar. The deposition rates measured by glancing incidence x-ray reflectometry and α-step measurements are 40 Å/s for Nb and 7 Å/s for CuNi in the center of the 75-mm wafer. The CuNi thickness was also determined at different positions on the substrate where several junctions are simultaneously patterned and we obtained a thickness range between 15 and 20 nm. The residual resistivity at 10 K for a thick niobium film is 8 $\mu\Omega$ cm corresponding to a mean free path of 5 nm and the transition temperature is 8.7 K. The residual resistivity for copper-nickel films is 50 $\mu\Omega$ cm corresponding to a mean free path about 1 nm and a diffusion coefficient of about 5 cm^2/s (using parameters of copper). The actual composition of the CuNi alloy was measured to be 48% of Ni by Rutherford backscattering on 5-nm and 10-nm films.

The magnetic properties of this $Cu_{52}Ni_{48}$ alloy have been measured using a superconductivity quantum interference device (SQUID) magnetometer on a 20-nm film in a Nb/CuNi/Nb trilayer and on a 200-nm film in a single CuNi layer. The temperature dependence of the magnetization is

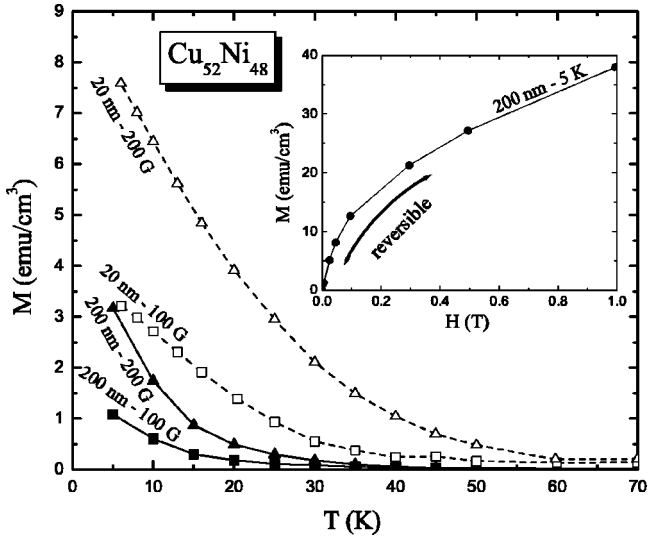

FIG. 9. Magnetization versus temperature for a 20-nm $Cu_{52}Ni_{48}$ layer in a Nb/CuNi/Nb trilayer and for a 200-nm $Cu_{52}Ni_{48}$ single layer. A magnetic field of 100 and 200 G is applied because the remanent magnetization is zero. Inset: reversible magnetization versus magnetic field at 5 K for the 200-nm $Cu_{52}Ni_{48}$ single layer.

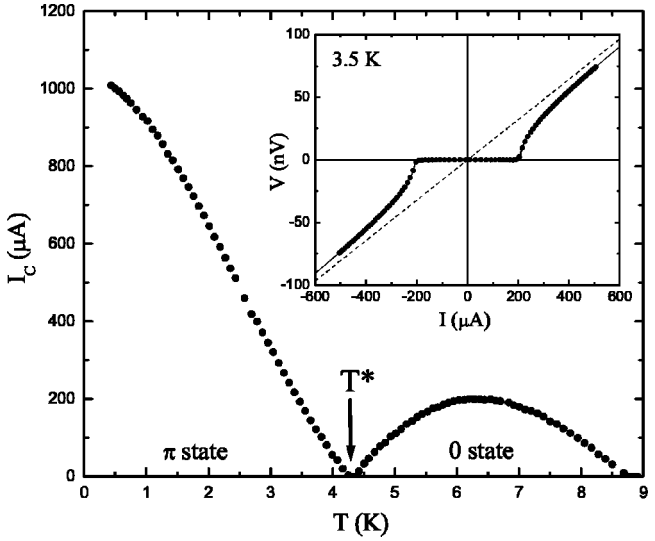

FIG. 10. Critical current versus temperature for a Nb/$Cu_{52}Ni_{48}$/Nb junction with $d=18$ nm. The cancellation at T^* corresponds to a change of the critical current sign and therefore to a crossover between a 0 state and a π state. Inset: voltage-current characteristic at 3.5 K (the solid line is a fit using the RSJ model and the dashed line represents the normal resistance).

shown in Fig. 9 under parallel magnetic fields of 100 G and 200 G. The Curie temperature is about 35 K for the trilayer and 20 K for the single layer. The magnetic-field dependence of the magnetization at 5 K is shown in the inset of Fig. 9 for the 200-nm single layer. The saturation magnetization can be extrapolated to 50 emu/cm^3 which corresponds to a magnetic moment of $0.06\mu_B$/atom. Bulk alloys of the same composition have similar characteristics with a Curie temperature of 23 K and a magnetic moment of $0.041\mu_B$/atom.[28] The exchange energy of bulk alloys has been calculated as a function of the concentration between 100% and 70% of Ni (Ref. 29) and a linear extrapolation for 48% (both the Curie temperature and the magnetic moment depend linearly on the concentration) indicates a value $E_{ex}\approx 12$ meV which is about ten times larger than the superconducting gap of niobium.

An important property of our $Cu_{52}Ni_{48}$ films is the absence of hysteresis, there is no measurable remanent magnetization, the magnetic behavior is perfectly reversible. This property indicates a very weak ferromagnetism close to the superparamagnetic behavior that occurs at 45% of Ni in bulk alloys.[28,30] In this regime the magnetic correlations are not long range any more, the direction of the magnetization can vary spatially without domain wall and the total magnetic moment can freely adjust to zero when the external field is removed. The characteristic length of these magnetic fluctuations is a few hundred atoms, close to the superconducting coherence length and the thickness of the barrier, so that the exchange energy is just uniform on the size of the Andreev bound states which carry the supercurrent through the junction.

B. Measurements of the critical current

The device is thermally coupled to the mixing chamber of a dilution refrigerator and electrically connected to a carefully filtered current source. The voltage between the superconducting electrodes is measured with a very sensitive setup since the characteristic voltage is a few nanovolts. A small fraction of the bias current flows into a parallel circuit containing a known resistance of 80 mΩ (much larger than the resistance of the junction) and a SQUID sensor which measures the derived current. The voltage across the junction is simply the product of this current by the resistance.

First we present the results obtained on a junction with a CuNi thickness about 18 nm and then we will consider different thicknesses. The voltage-current characteristic at 3.5 K is shown in the inset of Fig. 10 and is well described by the resistively shunted junction (RSJ) model in agreement with the low resistance and low capacitance of the junction.[31] The normal resistance $R_N=1.6\times10^{-4}$ Ω is close to the intrinsic CuNi layer resistance obtained from the resistivity and this indicates a good interface transparency. The critical current is measured continuously with a feedback method when temperature and magnetic field are varied. The temperature dependence is shown in Fig. 10 and presents a very unusual behavior with a cancellation at $T^*=4.3$ K where the voltage-current characteristic is a straight line going through the origin. This behavior corresponds to the crossover discussed extensively in the previous part with a sign in the current-phase relation that changes from negative at low temperature to positive above T^* and leads to the corresponding change from a π state to a 0 state.

The negative value of the critical current below T^* cannot be measured using a single junction because the direction of the current is imposed by the current source. The direct determination of the sign requires a control of the phase difference ϕ between the two superconducting electrodes and can be achieved by putting the junction in a superconducting

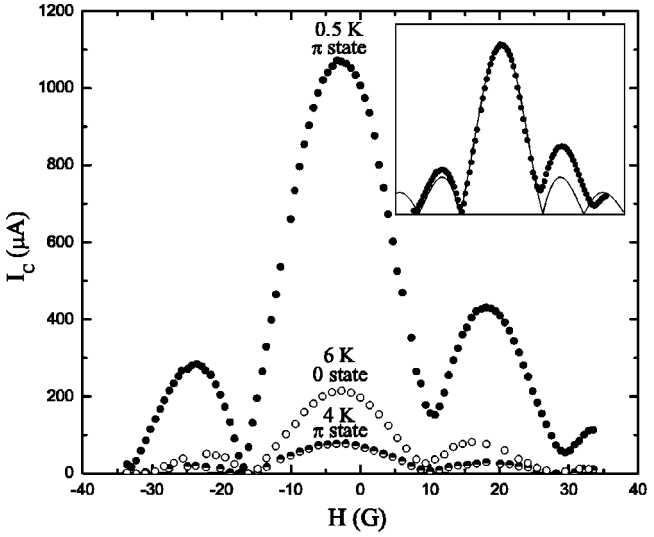

FIG. 11. Critical current versus magnetic field for a $Nb/Cu_{52}Ni_{48}/Nb$ junction with $d=18$ nm. These curves do not move with temperature and the critical current disappears completely (for all fields) at the crossover temperature of 4.3 K. Inset: comparison with the ideal Fraunhofer diffraction pattern (solid line).

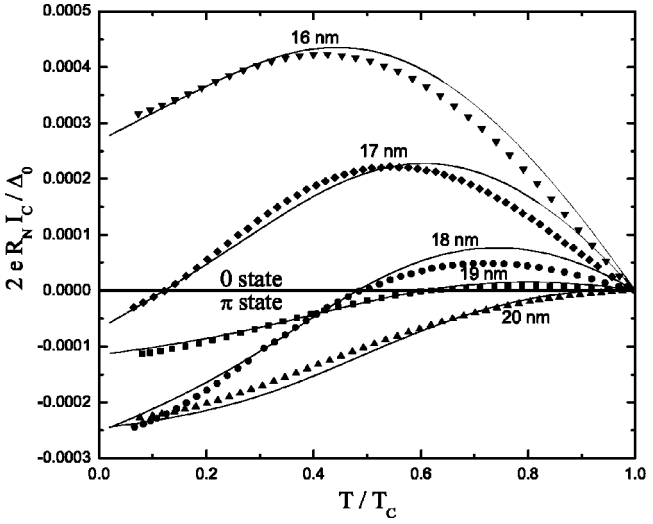

FIG. 12. Critical current versus temperature for $Nb/Cu_{52}Ni_{48}/Nb$ junctions with $d=16$–20 nm. The critical current is normalized and plotted with a negative sign for the π ground states. The solid lines are the theoretical curves obtained for each thickness by adjusting the exchange energy and the spin-flip length (Sec. V B) in order to fit the experimental data. $E_{ex}(0)$ was found in the range 6.8–7.4 meV and L_{sf} in the range 2.4–2.7 nm.

loop. This experiment was done by Ryazanov *et al.*[7,8] who observed the same kind of temperature dependence in Nb/CuNi/Nb junctions with higher Ni concentrations and hysteretic magnetization curves. They placed five identical junctions in a double superconducting loop and observed an interference pattern shifted by half a flux quantum when the temperature is decreased below T^*. This result demonstrates unambiguously that the sign of the current-phase relation changes at T^* and is negative below. We will therefore call π state the temperature region below T^* and 0 state the region above.

The magnetic-field dependence of the critical current is shown in Fig. 11 at three different temperatures below and above T^*. These curves present only small distortions with respect to the ideal Fraunhofer diffraction pattern (inset) and are almost centered around zero magnetic field in agreement with the zero remanent magnetization observed by magnetic measurements. The periodicity is about 14 G and corresponds to an effective thickness $d+2\lambda_L \approx 140$ nm consistent with the London penetration depth of niobium. The position of these curves does not change with temperature, only the amplitude does, and the critical current at T^* is zero for all values of the field. This result proves that the vanishing critical current observed at T^* in Fig. 10 is not due to a shift of the diffraction curve caused by an internal magnetic induction. If it were the case a nonzero critical current should be recovered by adding an external magnetic field at T^*. The crossover is indeed not due to a *spatial* distribution of supercurrent that compensates to zero at a given magnetic flux, but to a *spectral* distribution of supercurrent that compensates to zero at a given value of the exchange energy together with a given thermal distribution of quasiparticles.

The amplitude of the critical current and the shape of the diffraction pattern always change between successive cooling and depend on the magnetic field present when the niobium becomes superconducting. The earth field and the bias current create vortices in the electrodes and the resulting inhomogeneous magnetic field distorts the diffraction patterns of the junction. However, the crossover temperature T^* has always the same value because it is an intrinsic property which is independent of the magnetic field.

We compare now different junctions with CuNi thicknesses between 16 and 20 nm and show in Fig. 12 the temperature dependence of their critical current plotted with a negative sign when the ground state is supposed to be π. A crossover in temperature is obtained only for thicknesses between 17 and 19 nm, thinner junctions are always in the 0 state and thicker junctions always in the π state. This behavior was expected and confirms that the 0 and π states correspond, respectively, to the high- and low-temperature regions. When the thickness is small, the Thouless energy is large and the exchange energy becomes insufficient to shift the Andreev spectrum, so the ground state is the usual 0 state. The 16 nm junction behaves however differently from an usual Josephson junction since the critical current has a maximum at finite temperature. This indicates the presence of a negative supercurrent density which is close to the Fermi level and is suppressed when the temperature increases. The 20-nm junction has no crossover but the curvature of its critical current close to T_c is also unusual compared to the linear behavior of short junctions. This temperature dependence results from the combined effect of the superconducting gap that closes at T_c and a crossover to a 0 state that would have occurred at a temperature just above T_c.

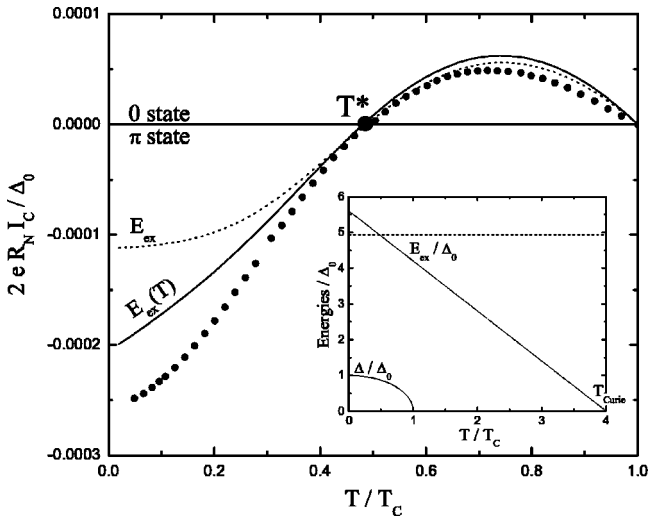

FIG. 13. Temperature dependence of the critical current for $d = 18$ nm (normalized and plotted with a negative sign below the crossover) compared with the theoretical model with a constant (dotted line) or temperature dependent (solid line) exchange energy as shown in the inset. The spin-flip scattering (Sec. V B) has been included with $L_{sf} = 3.1$ nm (dotted line) and 2.6 nm (solid line).

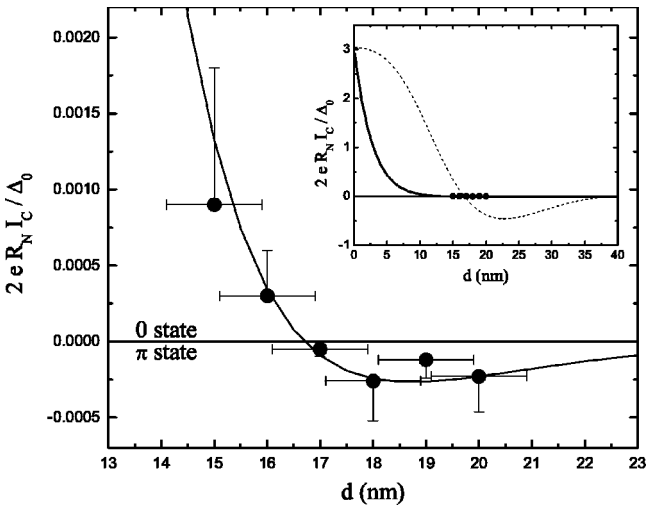

FIG. 14. Critical current of $Nb/Cu_{52}Ni_{48}/Nb$ junctions at zero temperature versus CuNi thickness compared to the theoretical model with $E_{ex}(0) = 7.2$ meV and a spin-flip length $L_{sf} = 2.7$ nm (solid line). Inset: same graph on a larger scale, plus the theoretical curve without spin-flip scattering (dashed line).

V. COMPARISON WITH THE THEORETICAL MODEL

A. Discussion of the temperature dependence

First we consider the 18-nm junction and try to reproduce its temperature behavior with a crossover at $T^* = 4.3$ K using the theoretical model of Sec. III. Three parameters are known: the normal resistance $R_N = 1.6 \times 10^{-4}\ \Omega$, the Thouless energy $E_{Th} = 1$ meV, and the superconducting gap $\Delta_0 = 1.3$ meV. The experimental critical current is plotted in Fig. 13 together with the theoretical curve using a constant exchange energy $E_{ex} = 6.4$ meV (dotted line). Both are expressed in terms of the normalized parameter $2eR_N I_C/\Delta_0$ but the amplitude of the theoretical curve has been strongly reduced to be comparable with the experimental one: the origin of this extremely weak supercurrent will be analyzed in the following section.

The saturation at low temperature is a general behavior: it occurs below about $0.2\,T_c$ for short junctions and below the Thouless energy for long S/N/S junctions. However, this saturation is not (or much less) present in our S/F/S junction because the exchange energy is still temperature dependent at low temperature. This dependence was reported for bulk CuNi alloys[32] and our own magnetic measurements (Fig. 9) also show that the magnetization is not saturated at 5 K and is still increasing linearly. For this reason we consider now the model already discussed in Sec. III with a temperature-dependent exchange energy $E_{ex}(T)$. Using a linear dependence and a Curie temperature of 35 K, this model reproduces better the experimental behavior at low temperature.

The different types of curves measured for different CuNi thicknesses can be reproduced with an exchange energy at zero temperature of about 7 meV (Fig. 12) using the same linear dependence for $E_{ex}(T)$ as before. As already mentioned, the theoretical amplitudes have to be strongly reduced to fit the experimental data: the physical origin of this reduction is explained in the following.

B. Discussion of the critical current amplitude

The large discrepancy between the measured amplitude and the model cannot be explained by the interface transparency because the barrier parameter $\Gamma_b = 0.3$, deduced from the normal resistance $R_N = 1.6 \times 10^{-4}\ \Omega = (1 + 2\Gamma_b)\rho d/\mathcal{S}$, is too small to have such an influence.[25] This good interface quality is achieved by an *in situ* deposition of the Nb/CuNi/Nb trilayer which avoids any contamination of the interface. Moreover, the small spin polarization of this very dilute magnetic alloy cannot reduce significantly the probability of the Andreev reflection as it is expected to do with high Curie temperature ferromagnets where the densities of states per spin are not equal.[33]

In the theoretical model we neglected any inelastic and decoherent process because the typical thickness of S/F/S junctions is usually quite small. However, our CuNi alloy has a superparamagnetic behavior which indicates that the magnetic moments can fluctuate easily and induce a large spin-flip scattering. This process destroys a large number of Andreev pairs and reduces therefore the supercurrent amplitude. However, the surviving pairs still form bound states whose spectrum depends on the exchange energy and the π state is not destroyed.

This process can be qualitatively taken into account by simply adding an exponential decay $\exp(-d/L_{sf})$ with a spin-flip scattering length L_{sf}. The maximum critical current at zero temperature is plotted in Fig. 14 as a function of the thickness and is well reproduced by the model with $E_{ex} = 7.2$ meV and $L_{sf} = 2.7$ nm. The error bars on the critical current indicate that higher values may be possible since we observed some changes depending on cooling conditions (see Sec. IV) typically by a factor of 2. The very small value

obtained for the spin-flip length can be compared to the 7.5 nm measured in the $Cu_{77}Ni_{23}$ alloy which is not magnetic at all, only because of the spin-orbit coupling.[34] It is therefore not unrealistic to have a shorter value in our superparamagnetic alloy.

The spin-flip scattering can also be directly included in the equations and this can be done easily in the linearized case by changing ϵ into $\epsilon + i\gamma_{sf}$ in the second term of Eq. (10), but not in the term containing the gap where $\gamma = 0^+$. This new theoretical expression reproduces the experimental data with almost the same spin-flip length $L_{sf} = \sqrt{\hbar D/\gamma_{sf}} = 2.5$ nm. However, it requires a different exchange energy $E_{ex} = 20$ meV because the shift of the Andreev bound states is now intrinsically coupled to the spin-flip scattering process.

VI. CONCLUSION

We have explained the π state of S/F/S junctions by a shift of the Andreev bound states in order to provide a better insight into the microscopic mechanism of this effect. The spectral supercurrent density in the diffusive regime has been calculated and used to interpret the origin of the $0-\pi$ crossover in temperature. We have presented some critical current measurements of $Nb/Cu_{52}Ni_{48}/Nb$ junctions where the barrier has a superparamagnetic behavior. In a small range of barrier thickness the critical current cancels out as a function of temperature when the ground state changes from 0 state to a π state. Our theoretical model can reproduce these experimental results by including a temperature-dependent exchange energy and a large spin-flip scattering.

ACKNOWLEDGMENTS

We thank A. Buzdin, M. Aprili, M. Houzet, I. Baladié, A. Vedyayev, and V. Mineev for stimulating discussions and D. Jalabert for RBS measurements.

*Present address: Department of Nanoscience, Delft University of Technology, Lorentzweg 1, 2628 CJ Delft, The Netherlands.

[1] L.N. Bulaevskiĭ, V.V. Kuziĭ, and A.A. Sobyanin, Pis'ma Zh. Eksp. Teor. Fiz. **25**, 314 (1977) [JETP Lett. **25**, 290 (1977)].
[2] A.I. Buzdin, L.N. Bulaevskiĭ, and S.V. Panyukov, Pis'ma Zh. Eksp. Teor. Fiz. **35**, 147 (1982) [JETP Lett. **35**, 178 (1982)].
[3] A.I. Buzdin and M.Y. Kupriyanov, Pis'ma Zh. Eksp. Teor. Fiz. **53**, 308 (1991) [JETP Lett. **53**, 321 (1991)].
[4] H.K. Wong, B.Y. Jin, H.Q. Yang, J.B. Ketterson, and J.E. Hilliard, J. Low Temp. Phys. **63**, 307 (1986).
[5] J.S. Jiang, D. Davidović, D.H. Reich, and C.L. Chien, Phys. Rev. Lett. **74**, 314 (1995).
[6] T. Mühge, N.N. Garif'yanov, Y.V. Goryunov, G.G. Khaliullin, L.R. Tagirov, K. Westerholt, I.A. Garifullin, and H. Zabel, Phys. Rev. Lett. **77**, 1857 (1996).
[7] V.V. Ryazanov, V.A. Oboznov, A.Y. Rusanov, A.V. Veretennikov, A.A. Golubov, and J. Aarts, Phys. Rev. Lett. **86**, 2427 (2001).
[8] V.V. Ryazanov, V.A. Oboznov, A.V. Veretennikov, and A.Y. Rusanov, Phys. Rev. B **65**, 020501 (2001).
[9] T. Kontos, M. Aprili, J. Lesueur, F. Genêt, B. Stephanidis, and R. Boursier, Phys. Rev. Lett. **89**, 137007 (2002).
[10] W. Guichard, M. Aprili, O. Bourgeois, T. Kontos, J. Lesueur, and P. Gandit, Phys. Rev. Lett. **90**, 167001 (2003).
[11] I.O. Kulik, Zh. Eksp. Teor. Fiz. **57**, 1745 (1969) [Sov. Phys. JETP **30**, 944 (1970)].
[12] F.K. Wilhelm, G. Schön, and A.D. Zaikin, Phys. Rev. Lett. **81**, 1682 (1998).
[13] T.T. Heikkilä, F.K. Wilhelm, and G. Schön, Europhys. Lett. **51**, 434 (2000).
[14] J. Bardeen, L.N. Cooper, and J.R. Schrieffer, Phys. Rev. **108**, 1175 (1957).
[15] M. Tinkham, *Introduction to Superconductivity*, 2nd ed. (McGraw-Hill, New York, 1996).
[16] A.F. Andreev, Zh. Eksp. Teor. Fiz. **46**, 1823 (1964) [Sov. Phys. JETP **19**, 1228 (1964)].
[17] E.A. Demler, G.B. Arnold, and M.R. Beasley, Phys. Rev. B **55**, 15 174 (1997).
[18] A.F. Andreev, Zh. Eksp. Teor. Fiz. **49**, 655 (1965) [Sov. Phys. JETP **22**, 455 (1966)].
[19] C. Ishii, Prog. Theor. Phys. **44**, 1525 (1970).
[20] J. Bardeen and J.L. Johnson, Phys. Rev. B **5**, 72 (1972).
[21] A. Furusaki and M. Tsukada, Phys. Rev. B **43**, 10 164 (1991).
[22] T. Kontos, M. Aprili, J. Lesueur, and X. Grison, Phys. Rev. Lett. **86**, 304 (2001).
[23] S.K. Yip, Phys. Rev. B **58**, 5803 (1998).
[24] K.D. Usadel, Phys. Rev. Lett. **25**, 507 (1970).
[25] M.Y. Kupriyanov and V.F. Lukichev, Zh. Eksp. Teor. Fiz. **94**, 139 (1988) [Sov. Phys. JETP **67**, 1163 (1988)].
[26] J.J.A. Baselmans, A.F. Morpurgo, B.J. van Wees, and T.M. Klapwijk, Nature (London) **397**, 43 (1999).
[27] V.V. Ryazanov, V.A. Oboznov, A.V. Veretennikov, A.Y. Rusanov, A.A. Golubov, and J. Aarts, Usp. Fiz. Nauk **171**, 81 (2001).
[28] T.J. Hicks, B. Rainford, J.S. Kouvel, G.G. Low, and J.B. Comly, Phys. Rev. Lett. **22**, 531 (1969).
[29] F. Brouers, A.V. Vedyayev, and M. Giorgino, Phys. Rev. B **7**, 380 (1973).
[30] J.P. Perrier, B. Tissier, and R. Tournier, Phys. Rev. Lett. **24**, 313 (1970).
[31] K.K. Likharev, Rev. Mod. Phys. **51**, 101 (1979).
[32] S.A. Ahern, M.J.C. Martin, and W. Sucksmith, Proc. R. Soc. London, Ser. A **248**, 145 (1958).
[33] M.J.M. de Jong and C.W.J. Beenakker, Phys. Rev. Lett. **74**, 1657 (1995).
[34] S.-Y. Hsu, P. Holody, R. Loloee, J.M. Rittner, W.P. Pratt, and P.A. Schroeder, Phys. Rev. B **54**, 9027 (1996).